

Clean High-Energy Density Renewable Power Generation Systems With Soft-Switching Sliding Mode Control Laws

Trevor C. Smith¹ and Sergey Edward Lyshevski²

¹Harris Corporation, Rochester, NY 14618

²Department of Electrical and Microelectronic Engineering, Rochester Institute of Technology, Rochester, NY 14623

E-mail: Sergey.Lyshevski@mail.rit.edu Web: <http://people.rit.edu/seleee/>

Abstract - This paper reports the design, analysis, evaluation and characterization of closed-loop *clean* renewable power generation systems. For the aforementioned multi-input/multi-output systems, we design proportional-integral and *soft-switching* sliding mode control laws to guarantee: (1) Efficient mechanical-to-electrical, electrical-to-electrical and electrical-to-chemical energy conversions; (2) Enabling wind- or hydro-energy harvesting capabilities; (3) Optimal dynamics, robustness and stability. The prototypes of portable high-energy-density power systems were tested, characterized and evaluated. We advanced energy sources, enabled electric machinery, and improved power electronics solutions. Linear and nonlinear control algorithms were designed, implemented, and verified. The developed closed-loop *clean* power generation systems were tested in enhanced operating envelopes. These scalable systems can be used as mini-scale, *light-* and *medium-*duty auxiliary, portable and self-sustained power systems in various applications, such as, aerospace, automotive, biotechnology, biomedical, communication, marine, robotics, etc.

I. INTRODUCTION

There is a need to advance and enable auxiliary and portable power systems for various civilian, security, military and other applications. Though viable solutions have been found and reported [1-5], current advances in engineering and technology provide enabling inroads at the component and system levels. The advanced solutions must be applied to design and control *clean* power generation, energy harvesting and energy storage systems which must guarantee high power and energy densities, efficiency, robustness, safety, reliability, scalability and sustainability [6]. To ensure re-design features and adaptation, we develop a modular system organization which is applicable to a wide class of auxiliary and portable power systems. The proposed system integrates:

1. Turbine (or other prime mover) which rotates a radial- or axial-topology permanent-magnet synchronous generator at variable angular velocity depending on flow rate, speed and load.
2. Power electronic module with controllable/uncontrollable rectifier, PWM converter, filters, controllers and charger.
3. Energy storage unit, e.g., rechargeable battery, supercapacitor, or other devices.

For the aforementioned multi-input/multi-output (MIMO) system, proportional-integral (PI) and *soft-switching* sliding mode control laws are synthesized, implemented and validated. The designed control algorithms ensure *optimal* or *near-optimal* performance.

Our major efforts are focused to guarantee overall consistency, cohesiveness and coherency of various design tasks, solutions and possible technologies. For nonlinear

MIMO systems, the concepts, findings and designs are substantiated by performing experimental studies, verification, testing and characterization at the component, subsystem and system levels. By using relevant application-specific adjustments, the proposed closed-loop power generation systems ensure enabling performance, specified capabilities, affordability and sustainability in various applications. The prototypes of integrated power generation systems are evaluated in expanded operating envelopes. It is found that high power and energy densities, high efficiency, robustness and other enabling capabilities are achieved due to the use of advanced system organizations.

The results and solutions are scalable from micro (starting from μW), to *light-* and *medium-*duty auxiliary and portable power and energy systems. This paper further enables engineering solutions and technology frontiers by applying the most advanced recent theoretical findings of electro-mechanics, electronics, control theory, nonlinear MIMO systems design, optimization, etc. Highly efficient energy conversion is ensured by using designed control laws to control a controllable converter and charger.

II. POWER GENERATION, ENERGY HARVESTING AND ENERGY STORAGE SYSTEMS

Enabling power generation systems are designed for various harsh environment applications, such as aerospace, submersible, etc. The proposed *clean* power generation system consists of energy harvesting, energy conversion and energy storage subsystems which are comprised of: (1) High-efficiency turbine or other prime mover; (2) High power density permanent-magnet brushless synchronous generator; (3) Power electronic module; (4) Energy storage unit.

The power electronic module includes: (i) Controlled or uncontrolled rectifier; (ii) Controllable dc/dc PWM converter; (iii) Filters; (iv) Controllable charger; (v) Controllers; (vi) Signal conditioning and monitoring circuitry; etc. The electrical energy can be stored by high-energy-density rechargeable batteries or super-capacitors (double-layer capacitors). This power generation system utilizes a minimal-complexity modular organization as reported in Figure 1.

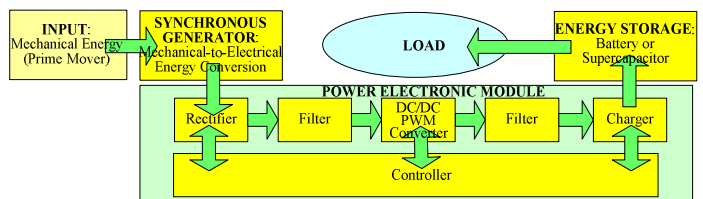


Figure 1. Functional block-diagram: Modular organization of power generation system

As energy storage solutions, we examine supercapacitors and advanced rechargeable batteries. The system design and development includes various fundamental tasks such as: (i) Control and optimization of energy generation and conversion; (ii) Efficient energy storage; (iii) Component- and system-level matching, utilization, integration and complementarity; (iv) Design of high-performance generators; (v) Synthesis of controllable rectifiers, converters and chargers; (vi) Optimization of charging profiles to ensure optimal charging; (vii) High-fidelity analysis, nonlinear design and multi-objective optimization; (viii) Verification, testing, characterization and evaluation; etc.

To ensure an optimal design and enable an expanded operating envelope, a turbine rotor may house permanent magnets forming an integrated turbine-generator unit. The coated rear-earth *hard* magnets, encapsulated in protecting polymers, are embedded in the turbine aperture. The generator's stator aperture with windings and a power electronic module are contained in a sealed package. The induced phase voltages are supplied to a rectifier, which converts *ac* voltage to *dc* voltage. The angular velocity of the turbine and generator varies. The varying induced voltage can be stabilized by using controllable rectifier and converter. The *LC* filters are aimed to attenuate undesirable voltage and current chattering, spikes and ripples. The stabilized *dc* voltage is supplied to a charger which charges the battery or supercapacitor using the specified mode within optimal current-voltage profiles. The PWM converter and charger are controlled by using the PI and *soft-switching* algorithms. The synthesized control laws are implemented using analog IC schemes and components. It is illustrated that the power generation, energy conversion and energy storage are adequately controlled and effectively optimized by controlling the PWM converter and charger.

III. SYNCHRONOUS GENERATOR

Various permanent-magnet brushless synchronous generators were designed and tested. We analyze multi-pole commercially available and newly designed generators. The prime mover angular velocity and applied torque predefine the rated and peak power, current, induced voltage, angular velocity and other descriptive quantities. For multi-pole generators, one has

$$T_{PM} = T_{emL} + T_{friction}, \quad T_{emL} = \frac{1}{2} P T_{eL}$$

where T_{PM} is the applied torque of the prime mover (turbine); T_{eL} is the electromagnetic load torque of the synchronous generator; P is the number of poles.

The mechanical and electrical angular velocities of prime mover and generator are related as

$$\omega_m = 2 \omega_e / P,$$

where ω_m and ω_e are the mechanical and electrical angular velocities of prime mover and generator.

These multi-pole generators guarantee high torque and power densities due to high electrical angular velocity. The permanent-magnet synchronous generators induce phase voltages as induced *emf*. One has

$$emf = \oint_l \mathbf{E} \cdot d\mathbf{l} = \oint_l (\mathbf{v} \times \mathbf{B}) \cdot d\mathbf{l} - \oint_s \frac{\partial \mathbf{B}}{\partial t} \cdot d\mathbf{s}.$$

High-fidelity analysis, nonlinear design and multi-objective electromagnetic optimization of synchronous machines are reported in [6-9]. Permanent-magnet synchronous generators (which are available from μW to sub-megawatt) guarantee the best performance as compared to other dc and ac electric machines.

The images of some examined high-performance axial and radial topology generators with the outer diameter from ~ 2 mm to ~ 10 cm are documented in Figure 2. These medium- and high-speed generators (~ 100 to $10,000$ rad/sec, ~ 1 mW to ~ 100 W). For these generators, the windings can be placed in the stationary sealed waterproof case. In radial and axial topology generators, the segmented permanent magnets are used to form ring- and disk-shaped magnets with various outer and inner diameters matching the turbine rotor housing. The Pelton turbine is utilized for submersible applications. The vanes sizing, geometry and curvature are defined by performing an application-specific design to ensure maximum efficiency within the operating envelope. An integrated turbine-generator unit, shown in Figure 2, contains permanent magnets on the turbine rotor, thereby guarantying a unique utilization of the turbine structure. This solution ensures superior performance and robustness.

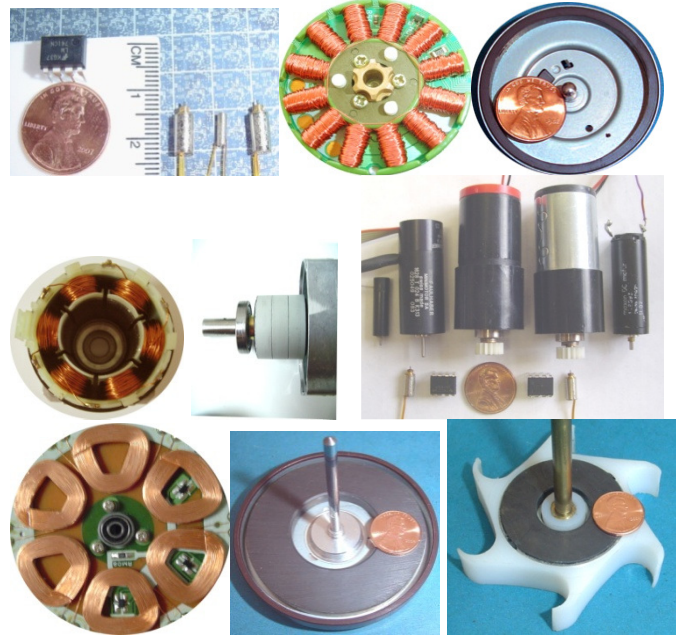


Figure 2. High-performance permanent-magnet radial and axial topology synchronous generators: From 2 mm to ~ 10 cm rotor outer diameter, ~ 1 mW to 100 W, ~ 100 to $10,000$ rad/sec. Windings are on the stator, while permanent magnets are on the rotor allowing one to design turbines with permanent magnets

IV. POWER ELECTRONIC MODULE

Two- and three-phase *ac* to *dc* controlled and uncontrolled rectifiers with a *LC* output filter are used to rectify the induced *ac* phase voltages to a *dc* voltage. To charge the rechargeable battery or supercapacitor, a specialized charger must be used. The input voltage to the charger must be stabilized using the

PWM converter. Various controlled *buck*, *boost*, *buck-boost* and *flyback* PWM converters were synthesized and utilized to ensure high efficiency. For one-, two- and four-quadrant converters, the operating principle is based on the changing of a duty ratio (duty cycle) [6-10]. For the considered systems, controllable one- and two-quadrant *buck-boost* and *flyback* PWM converters with PI and *soft-switching* control laws are studied. The voltage can be stabilized in the full operating envelope. The *LC* output filter attenuates the voltage and current chattering and ripples thereby enabling performance and improving efficiency.

To solve a wide range of challenging problems one must utilize the most advanced hardware solutions. The proposed system coherently integrates the major components which are designed and chosen using the *first principles* of electrical and mechanical engineering. The power generation, energy conversion, voltage induction, energy storage and other inherent mechanisms are consistently studied allowing a systematic design. One integrates a prime mover, generator and electronics using the requirements and specifications. By performing the application-specific synthesis, we define and optimize components and subsystems within requirements and specification to ensure the best *achievable* capabilities. All system components must be selected using a consistent systematic analysis.

V. MATHEMATICAL MODEL OF CLEAN POWER GENERATION SYSTEMS

This section reports various aspects of modeling as pertained to power generation systems. Consider a system with a three-phase brushless generator, uncontrollable rectifiers, dc/dc *buck-boost* converter, bandpass *LC* filters, battery chargers and rechargeable battery.

A high-fidelity mathematical model of three-phase permanent-magnet synchronous generators is reported in [9]. A prime mover applies the torque T_{PM} rotating a generator with the mechanical angular velocity $\omega_m = 2\omega/P$. The differential equations of a round-rotor permanent-magnet synchronous generator are [6-9]

$$0 = \mathbf{r}_s \mathbf{i}_{abc s} + \frac{d\boldsymbol{\Psi}_{abc s}}{dt} = \mathbf{r}_s \mathbf{i}_{abc s} + \mathbf{L}_s \frac{d\mathbf{i}_{abc s}}{dt} + \frac{d\boldsymbol{\Psi}_m}{dt},$$

$$\boldsymbol{\Psi}_{abc s} = \begin{bmatrix} \psi_{as} \\ \psi_{bs} \\ \psi_{cs} \end{bmatrix} = \begin{bmatrix} L_s + \bar{L}_m & -\frac{1}{2}\bar{L}_m & -\frac{1}{2}\bar{L}_m \\ -\frac{1}{2}\bar{L}_m & L_s + \bar{L}_m & -\frac{1}{2}\bar{L}_m \\ -\frac{1}{2}\bar{L}_m & -\frac{1}{2}\bar{L}_m & L_s + \bar{L}_m \end{bmatrix} \begin{bmatrix} i_{as} \\ i_{bs} \\ i_{cs} \end{bmatrix} + \boldsymbol{\Psi}_m \begin{bmatrix} \sum_{n=1}^{\infty} a_n \sin^{2n-1} \theta_r \\ \sum_{n=1}^{\infty} a_n \sin^{2n-1} (\theta_r - \frac{2}{3}\pi) \\ \sum_{n=1}^{\infty} a_n \sin^{2n-1} (\theta_r + \frac{2}{3}\pi) \end{bmatrix}$$

$$\frac{d\omega_r}{dt} = -\frac{P^2 \boldsymbol{\Psi}_m}{4J} \begin{bmatrix} i_{as} \\ i_{bs} \\ i_{cs} \end{bmatrix} \sum_{n=1}^{\infty} (2n-1) a_n \cos \theta_r \sin^{2n-2} \theta_r$$

$$+ i_{bs} \sum_{n=1}^{\infty} (2n-1) a_n \cos (\theta_r - \frac{2}{3}\pi) \sin^{2n-2} (\theta_r - \frac{2}{3}\pi)$$

$$+ i_{cs} \sum_{n=1}^{\infty} (2n-1) a_n \cos (\theta_r + \frac{2}{3}\pi) \sin^{2n-2} (\theta_r + \frac{2}{3}\pi) \Big] - \frac{B_m}{J} \omega_r + \frac{P}{2J} T_{PM},$$

$$\frac{d\theta_r}{dt} = \omega_r, \quad (1)$$

where $\mathbf{i}_{abc s} = [i_{as} \ i_{bs} \ i_{cs}]^T$ and $\boldsymbol{\Psi}_{abc s} = [\psi_{as} \ \psi_{bs} \ \psi_{cs}]^T$ are the currents and flux linkages; $d\boldsymbol{\Psi}_m/dt$ is the motional *emf* which represents the induced phase voltages $\mathbf{u}_{abc s} = [u_{as} \ u_{bs} \ u_{cs}]^T$; ω_r

and θ_r are the electrical angular velocity and displacement; \mathbf{r}_s is the diagonal matrix of phase resistances; \mathbf{L}_s is the symmetric matrix of inductances; $\boldsymbol{\Psi}_m$ is the vector of flux linkages due to phase windings and permanent magnet time-varying and displacement-dependent magnetic coupling; $\boldsymbol{\Psi}_m$ and a_n are the constants; J and B_m are the equivalent moment of inertia and friction coefficient.

Using the *averaging* concept, the mathematical models of PWM converters are documented in [9, 10]. Using the state variables (voltage u_c , and, currents i_L and i_a) as well as control (the duty ratio d_D), for a one-quadrant *buck-boost* switching converter, we have

$$\frac{du_c}{dt} = \frac{1}{C} (i_L - i_a), \quad \frac{di_a}{dt} = \frac{1}{L_a} (u_c + r_c i_L - (r_a + r_c) i_a - E_a),$$

$$\frac{di_L}{dt} = \frac{1}{L} (-u_c - (r_L + r_c) i_L + r_c i_a - r_s i_L d_D + V_d d_D). \quad (2)$$

The duty ratio is regulated by the signal-level control voltage u_c . These u_c is bounded. In particular,

$$d_D = \frac{u_c}{u_{t \max}} \in [0 \ 1], \quad u_c \in [0 \ u_{c \max}], \quad u_{c \max} = u_{t \max}.$$

Two bandpass *LC* filters are easily modeled.

The resulting models for the LT1071 *buck-boost* converter (3 to 30 V, 3 A, 50 W) and PWM battery charger LT1510 (2 to 20 V, 1.5 A) can be derived. The aforementioned battery charger supports the *constant-current* and *constant-voltage* modes ensuring fast charging within optimal charging profiles for various rechargeable batteries such as lithium-ion, nickel-metal-hydride and nickel-cadmium.

In the governing equations of motion, the parameters vary. In particular, almost all parameters (resistances, permeability, permanent magnet susceptibility and other) are load-, temperature- and state-of-charge dependent. We define these parameters as $a_{ii}(\cdot)$ and $b_{jj}(\cdot)$. These parameter variations are bounded as

$$a_{iimin} \leq a_{ii}(z) \leq a_{iimax}, \quad a_{iimin} > 0, \quad a_{iimax} > 0,$$

$$\text{and } b_{jjmin} \leq b_{jj}(p) \leq b_{jjmax}, \quad b_{jjmin} > 0, \quad b_{jjmax} > 0.$$

Using (1), (2) and other components models, the studied dynamic system with uncertain parameters is given as

$$\dot{x}(t) = F_z(t, x, r, d, z) + B_p(t, x, p)u, \quad y = Hx, \quad (3)$$

$$e(t) = Nr(t) - y(t),$$

where $x \in X \subset \mathbb{R}^c$ is the state vector; $u \in U \subset \mathbb{R}^m$ is the control vector with the known closed admissible set $U = \{u \in \mathbb{R}^m \mid u_{\min} \leq u \leq u_{\max}, \quad u_{\max} > 0, \quad u_{\min} < 0\}$; $r \in R \subset \mathbb{R}^b$ and $y \in Y \subset \mathbb{R}^b$ are the reference and output vectors; $d \in D \subset \mathbb{R}^s$ is the disturbance vector; $z \in Z \subset \mathbb{R}^d$ and $p \in P \subset \mathbb{R}^k$ are the time-varying bounded uncertainties; $e \in E \subset \mathbb{R}^b$ is the tracking error; $F_z(\cdot)$ and $B_p(\cdot)$ are the nonlinear maps; $H \in \mathbb{R}^{b \times c}$ and $N \in \mathbb{R}^{b \times b}$ are the matrices.

The transient dynamics of system (3) can be modeled as

$$\dot{x}(t) = F_x(t, x, r, d) + B_x(t, x)u + \Xi(t, x, u, z, p). \quad (4)$$

The parameter variations are bounded. For the time-varying bounded uncertainties $z \in Z$ and $p \in P$ there exists a norm of $\Xi(t, x, u, z, p)$ such that $\|\Xi(t, x, u, z, p)\| \leq \rho(t, x)$, where $\rho(\cdot): \mathbb{R}_{\geq 0} \times \mathbb{R}_{\geq 0} \rightarrow \mathbb{R}_{\geq 0}$ is the continuous Lebesgue measurable function.

VI. SLIDING MODE CONTROL OF MIMO SYSTEMS

Sliding mode control is an enabling concept allowing one to design stabilizing and tracking control algorithms. Control laws can be designed to guarantee the evolution of system variables within the specified neighborhood of the *switching surface*. That is, the closed-loop dynamic behavior is tailored by a particular *switching surface* which should adequately map the component and system physics. The objective is to attain the system evolution within the state-space sub manifold (so-called *sliding manifold* or *switching surface*) as expressed as $\mathcal{U}(t,x)=0$ [11-15].

The hard-switching sliding control law is given as

$$u(t,x) = \text{sgn}[\mathcal{U}(t,x)]. \quad (5)$$

We design *soft-switching* continuous control laws with nonlinear *switching surfaces* [14]. Our goal is to synthesize a control law for system (3) such that the error vector $e(t)$ with $E_0 = \{e_0 \in \mathbb{R}^b\} \subset E \subset \mathbb{R}^b$ evolves in the specified closed set $S_\delta(\delta) = \{e \in \mathbb{R}^b : e_0 \in E_0, x \in X(X_0, U, R, D, Z, P), r \in R, d \in D, y \in Y, t \in [t_0, \infty)\}$ $\|e(t)\| \leq \rho_e(t, \|e_0\|) + \rho_r(\|r\|) + \rho_d(\|d\|) + \rho_y(\|y\|) + \delta, \delta \geq 0, \forall e \in E(E_0, R, D, Y), \forall t \in [t_0, \infty)\} \subset \mathbb{R}^b$,

where $\rho_e(\cdot) : \mathbb{R}_{\geq 0} \times \mathbb{R}_{\geq 0} \rightarrow \mathbb{R}_{\geq 0}$ is the *KL*-function; $\rho_r(\cdot) : \mathbb{R}_{\geq 0} \rightarrow \mathbb{R}_{\geq 0}$, $\rho_d(\cdot) : \mathbb{R}_{\geq 0} \rightarrow \mathbb{R}_{\geq 0}$ and $\rho_y(\cdot) : \mathbb{R}_{\geq 0} \rightarrow \mathbb{R}_{\geq 0}$ are the *K*-functions.

Singularity, chattering, sensitivity and degraded efficiency of the discontinuous (hard-switching) sliding control laws

$$u(t,x,e) = -G \text{sgn}[\mathcal{U}(t,x,e)] \quad (6)$$

have challenged the application of sliding mode algorithms.

A *soft-switching* tracking *admissible* control law for system (3) is given as [14]

$$u(t,x,e) = -G\phi[\mathcal{U}(t,x,e)], \quad G > 0, G \in \mathbb{R}^{m \times m}, u \in U, \quad (7)$$

where $\phi(\cdot)$ is the continuous real-analytic bounded function of class $C^k, k \geq 1$.

Example 6. 1. Using the hyperbolic tangent \tanh , one has

$$u(t,x,e) = u_{\max} \tanh^q v \quad \text{or} \quad u(t,x,e) = u_{\max} \tanh^q v,$$

where $q=1,3,5,\dots$ Furthermore, $u_{\min} \leq u(t,x,e) \leq u_{\max}$.

By applying the sigmoid function, we have

$$u(t,x,e) = u_{\max} \frac{1}{1 + e^{-a(v-b)}}, \quad 0 \leq u(t,x,e) \leq u_{\max}. \quad \blacksquare$$

The control law (7) is bounded, and, $u \in U$ for all $x \in X$ and $e \in E$ on $[t_0, \infty)$. The proposed *soft-switching* control algorithm is different from discontinuous (hard-switching) control algorithms [11-13]. Compared with hard-switching control laws, the advantages of the *soft-switching* continuous control are: (1) Enhanced stability; (2) Robustness; (3) Elimination of singularity and sensitivity; (4) Reduction or elimination of chattering (high frequency switching); (5) Enhanced functionality; etc. These advantages allow the designer to significantly expand operating envelopes, enhance robustness, and improve efficiency of controlled dynamic systems.

The closed-loop uncertain system (3) with (7) evolves in $XY(X_0, U, R, D, Z, P) = \{(x,y) \in X \times Y : x_0 \in X_0, u \in U, r \in R, d \in D, z \in Z, p \in P, t \in [t_0, \infty)\} \subset \mathbb{R}^c \times \mathbb{R}^b$.

The *soft-switching* sliding mode control law (7):

1. Drives the closed-loop system states $x(t)$ and tracking errors $e(t)$ to the equilibrium manifold;

2. Maintains the evolution of states and tracking errors within the equilibrium manifold defined by the *switching surface*.

The continuous sliding manifold is given by

$$M = \{(t,x,e) \in \mathbb{R}_{\geq 0} \times X \times E \mid v(t,x,e) = 0\} \\ = \bigcap_{j=1}^m \{(t,x,e) \in \mathbb{R}_{\geq 0} \times X \times E \mid v_j(t,x,e) = 0\} \quad (8)$$

The time-varying linear *switching surface* is

$$v(t,x,e) = [K_{ux}(t) \quad K_{ue}(t)] \begin{bmatrix} x(t) \\ e(t) \end{bmatrix} = K_{ux}(t)x(t) + K_{ue}(t)e(t) = 0. \quad (9)$$

A nonlinear *switching surface* is governed as

$$\begin{bmatrix} v_1(t,x,e) \\ \vdots \\ v_m(t,x,e) \end{bmatrix} = \begin{bmatrix} k_{ux11}(t) & \cdots & k_{ux1c}(t) & k_{ue11}(t) & \cdots & k_{ue1b}(t) \\ \vdots & & \vdots & \vdots & & \vdots \\ k_{uxm1}(t) & \cdots & k_{uxmc}(t) & k_{uem1}(t) & \cdots & k_{uemb}(t) \end{bmatrix} \begin{bmatrix} x_1(t) \\ \vdots \\ x_c(t) \\ e_1(t) \\ \vdots \\ e_b(t) \end{bmatrix} = 0 \\ v(t,x,e) = K_{vxc}(t,x,e) = 0, \quad \begin{bmatrix} v_1(t,x,e) \\ \vdots \\ v_m(t,x,e) \end{bmatrix} = \begin{bmatrix} K_{vxc1}(t,x,e) \\ \vdots \\ K_{vxcem}(t,x,e) \end{bmatrix} = 0. \quad (10)$$

The total derivative of the time-varying *switching surface* is expressed as

$$\frac{dv(t,x,e)}{dt} = \frac{\partial v(t,x,e)}{\partial t} + \frac{\partial v(t,x,e)}{\partial x} \dot{x}(t) + \frac{\partial v(t,x,e)}{\partial e} \dot{e}(t). \quad (11)$$

From (3) and (7), one finds

$$\frac{dv(t,x,e)}{dt} = \frac{\partial v}{\partial t} + \frac{\partial v(t,x,e)}{\partial x} \left[F_z(t,x,r,d,z) + B_p(t,x,p)u \right] \\ + \frac{\partial v(t,x,e)}{\partial e} \left[Nr(t) - HF_z(t,x,r,d,z) - HB_p(t,x,p)u \right]. \quad (12)$$

The *equivalent* control can be derived from

$$\frac{dv(t,x,e)}{dt} = 0. \quad (13)$$

The sufficient conditions for robust stability are formulated using the Lyapunov stability theory [14]. The Lyapunov stability theory is also applied to the closed-loop system (3) with linear or nonlinear PI control laws [14].

Theorem 6. 1. Consider the closed-loop system (3) with *soft-switching* tracking *admissible* sliding mode control (7) The state variable and tracking error vectors evolve in $XE(X_0, E_0, U, R, Y, D) \subset \mathbb{R}^c \times \mathbb{R}^b$. The *admissible* domain of robust stability and tracking $S_\delta(\delta) \subset \mathbb{R}^b$ is found using the criteria imposed on the Lyapunov function

$$\rho_1 \|x\| + \rho_2 \|e\| \leq V(t,x,e) \leq \rho_3 \|x\| + \rho_4 \|e\|, \\ \frac{dV(t,x,e)}{dt} \leq -\rho_5 \|x\| - \rho_6 \|e\|. \quad (14)$$

The robust tracking, stability, and disturbance attenuation in XE are guaranteed if $XE \subset S_\delta$ for given initial conditions ($x_0 \in X_0$ and $e_0 \in E_0$), control bounds $u \in U$, references $r \in R$, uncertainties $z \in Z$ and $p \in P$, and, disturbances $d \in D$. Furthermore, all solutions of the closed-loop system $x(\cdot) : [t_0, \infty) \rightarrow \mathbb{R}^c$, as well as evolutions $e(\cdot) : [t_0, \infty) \rightarrow \mathbb{R}^b$, are

robustly bounded. The convergence of the tracking error vector $e(\cdot):[t_0, \infty) \rightarrow \mathbb{R}^b$ to the $S_c(\delta)$ is guaranteed if $XE \subset S_c$. ■

VII. CLOSED-LOOP POWER GENERATION SYSTEM

Power generation systems are highly nonlinear MIMO system with varying parameters, unmodeled dynamics, etc. Using the Lyapunov stability theory and (7), we design the following PI and *soft-switching* control laws for the PWM converter and charger:

$$u_1(e) = -\phi_1(k_{p1}e_1 + \int k_{i1}e_1 dt), \quad (15)$$

$$u_2(e) = -\phi_2(k_{p2}e_2 + \int k_{i2}e_2 dt), \quad u_3(e) = -\phi_3(k_{p3}e_3 + \int k_{i3}e_3 dt),$$

and

$$u_1(e) = -\phi_1[\mathcal{U}(e_1, e_2, e_3, V_1)], \quad (16)$$

$$u_2(e) = -\phi_2[\mathcal{U}(e_1, e_2, e_3, V_2)], \quad u_3(e) = -\phi_3[\mathcal{U}(e_1, e_2, e_3, V_2)].$$

where k_{pj} and k_{ij} are the proportional and integral feedback gains; e_1 , e_2 and e_3 are the tracking errors, $e_1(t) = V_{r1}(t) - V_1(t)$, $e_2(t) = I_{r2}(t) - I_2(t)$, $e_3(t) = V_{r2}(t) - V_2(t)$, or, $e(t) = Nr(t) - y(t)$; $V_1(t)$, $V_2(t)$ and $I_2(t)$ are the outputs (voltages and current) of the controllable converter and charger.

For the charger, depending on the charging profile, the references are the current $I_{r2}(t)$ and voltage $V_{r2}(t)$.

The PI and *soft-switching* control algorithms (15) and (16) are the minimal-complexity control laws which are easy to implement. Using a continuous integrable bounded function \tanh , one can implement the designed control laws (15) and (16) using the instrumentation operational amplifiers, as well as build-in-the-chip ICs capabilities.

The feedback gain coefficients are found by using (14). For example, one solves

$$\frac{dV(x, e)}{dt} \leq -\|e\|. \quad (17)$$

We use the quadratic positive-definite Lyapunov function $V(x, e) = \frac{1}{2}x^T Kx + \frac{1}{2}v^T(e)K_v v(e)$. (18)

The PI control law is

$$u_1(e) = -\tanh(k_{p1}e_1 + k_{i1}\int e_1 dt), \quad u_2(e) = -\tanh(k_{p2}e_2 + k_{i2}\int e_2 dt), \quad u_3(e) = -\tanh(k_{p3}e_3 + k_{i3}\int e_3 dt). \quad (19)$$

This PI control scheme is implemented. The testing, characterization and verification are performed with different proportional and integral feedback gains. A fully functional power generation system is illustrated in Figure 3. At the rated and peak loads, the experimental results are documented in Figures 4 to 6. We examine an expanded operating envelope due to different loads (predefined by the battery state-of-charge and charging profile), angular velocity, temperature, etc. The operating envelope is mainly predefined by

$V_j \in [V_{j \min} \ V_{j \max}]$, $i_j \in [i_{j \min} \ i_{j \max}]$, $\text{SoC} \in [\text{SoC}_{\min} \ \text{SoC}_{\max}]$, $\omega_m \in [\omega_{m \min} \ \omega_{m \max}]$ and $T_j \in [T_{j \min} \ T_{j \max}]$.

Here, the subscript j denotes the voltages and currents of the generator, rectifier, converter and battery charger.

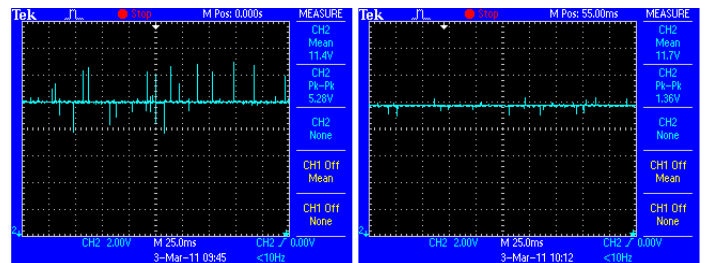
In the expanded operating envelope $\omega_m \in [50 \ 1000]$ rad/sec. Depending on the angular velocity of rotation, the output voltage of the rectifier varies from 5 V to 100 V. Figure 4.a documents the stabilized voltage after the *buck-boost* converter. We use the built-in analog PI controllers within the PWM converter and charger. The designed nonlinear control laws may be implemented using additional analog ICs. Figure 4.b reports that voltage and current spikes

and chattering are eliminated by using the LC output filter. Hence, the controlled PWM *buck-boost* converter regulates and stabilizes the output voltage to the desired value. An optimal operation is achieved, and, the voltage stabilization is ensured with $V_{\text{converter}} = 15.5$ V. The voltage is stabilized by a PWM converter at the rated and peak loads as illustrated in Figure 5. The resistive loads (15 and 5 ohms) were applied.

Figure 6 reports the voltage stabilization capabilities to the desired $V_{\text{converter}} = 15.5$ V at the rated ($I_{\text{converter}} = 1$ A) and peak ($I_{\text{converter}} = 3$ A) loads if generator rotates at varying angular velocity $\omega_m \in [200 \ 1000]$ rad/sec. In the expanded operating envelope, despite load and speed variations, we achieve $V_{\text{converter}} = 15.5 \pm 0.05$ V. The load depends on the battery state-of-charge, and, $i_{\text{converter}}$ and i_{charger} may not exceed 1.5 A which is a peak current. To create the peak and extreme loads, we use the resistive load R_L to emulate very high number of cells (or loads) within virtually inadequate configurations. Despite the peak and extreme loads, we are able to effectively charge these inadequate rechargeable battery packages or provide the specified power to the loads. The angular velocity of a prime mover decreases due to extremely high loading torque. These variations of $\Delta\omega_m$ may lead to the decrease of $V_{\text{converter}}$. Even at these extreme loads, at the low angular velocity of rotation (ω_m is less than 300 rad/sec), the proposed system is operational and functional. The experimental results are illustrated in Figure 7. We ensure an optimal or near-optimal charging profiles using the *constant-current*, *constant-voltage* and *varying voltage/current* modes and charging profiles. We examined different loads, distinct charging phases, and various charging profiles in an expanded operating envelope. Various lithium-ion batteries in different configurations were successfully charged guarantying robustness, high efficiency and superior capabilities. The efficiency of the power electronic module is found to be ~80%.



Figure 3. Electronic module of a high power density generation system



(a)

(b)

Figure 4. (a) Voltage stabilization at the output a *buck-boost* converter terminal at the rated load ($I_{\text{converter}} = 1$ A) if $\omega_m = 300$ rad/sec; (b) Attenuation of the voltage spikes ($I_{\text{converter}} = 1$ A, $\omega_m = 300$ rad/sec) using the output LC filter

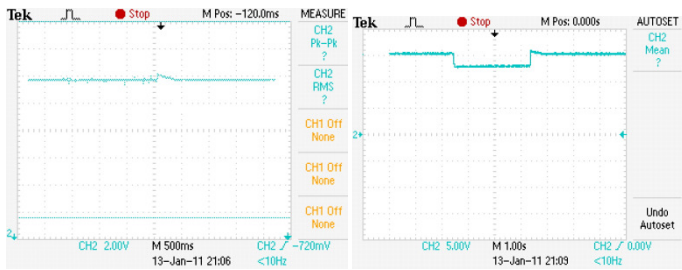


Figure 5. Voltage stabilization by a PWM *buck-boost* converter at the rated ($I_{\text{converter}}=1$ A) and peak ($I_{\text{converter}}=3$ A) loads if super loads are applied. We guarantee $V_{\text{converter}}=15.5\pm 0.05$ V.

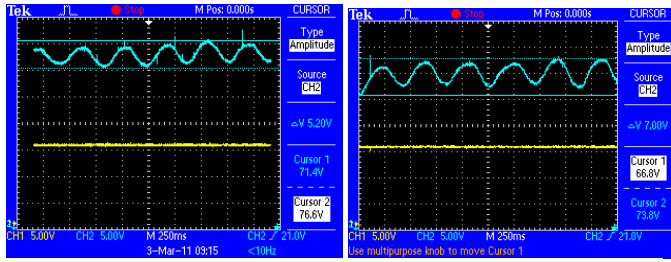


Figure 6. Voltage stabilization by a PWM *buck-boost* converter with varied input power and sinusoidal changes of angular velocity: Variation of the angular velocity, ω_m , is displayed on top, and the stabilized output voltage, $V_{\text{converter}}$, is displayed on the bottom. Here, $\omega_m \in [200 \ 1000]$ rad/sec, while $V_{\text{converter}}=15.5\pm 0.05$ V.

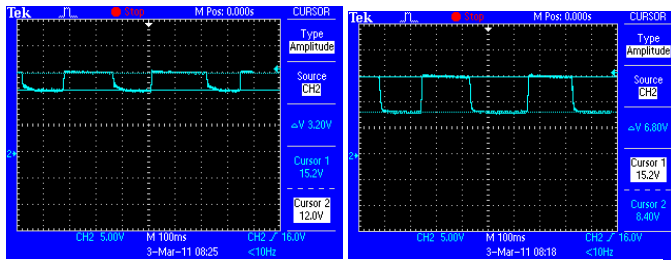


Figure 7. Voltage stabilization capabilities at the peak load ($I_{\text{converter}}=3$ A, $\omega_{m0}=300$ rad/sec, $\Delta\omega_m=50$ rad/sec), and, extreme load ($I_{\text{converter}}=4$ A, $\omega_{m0}=300$ rad/sec, $\Delta\omega_m=100$ rad/sec).

VIII. CONCLUSIONS

Our overall objective was to devise, design, build, demonstrate, verify and characterize innovative *clean* (emission and pollution free) power generation systems which include energy harvesting, energy conversion and energy storage subsystems. In order to ensure *optimal* or *near-optimal* performance and capabilities, we designed closed-loop systems. In particular, PI and *soft-switching* sliding mode control laws were designed and implemented for nonlinear MIMO systems with varying parameters. We advanced knowledge, engineering practice and technology for *clean* and renewable energy systems. The overall goal was to translate recent scientific discoveries, advanced engineering solutions and enabling inventions into technological developments and engineering breakthroughs. The overall and specific objectives and goals were accomplished.

This paper accelerated transformative basic, applied and technological advances in core areas which are of great significance. The proposed concept and system ensured a viable inroad for affordable pollution/emission-free energy

production (generation) with exceptional power- and energy-relevant implications due to:

1. Affordability and accessibility;
2. Efficiency and effectiveness;
3. Sustainability;
4. Safety and security;
5. Feasibility and flexibility;
6. Simplicity and adaptability;
7. Diversification of energy sources;
8. Ecology friendly *clean* (waste-free) technology.

REFERENCES

1. R. C. Bansal, T. S. Bhatti and D. P. Kothari, "On some of the design aspects of wind energy conversion systems," *Energy Conversion and Management*, vol. 43, issue 16, pp. 2175-2187, 2002.
2. S. M. Camporeale and V. Magi, "Streamtube model for analysis of vertical axis variable pitch turbine for marine currents energy conversion," *Energy Conversion and Management*, vol. 41, issue 16, pp. 1811-1827, 2000.
3. E. Hiraki, K. Yamamoto and T. Mishima, "An isolated bidirectional DC-DC soft switching converter for super capacitor based energy storage systems," *Proc. Conf. Power Electronics Specialists*, pp. 390-395, 2007.
4. N. Lior, "Advanced energy conversion to power," *Energy Conversion and Management*, vol. 38, issues 10-13, pp. 941-955, 1997.
5. S. C. Tripathy, M. Kalantar and N. D. Rao, "Wind turbine driven self-excited induction generator," *Energy Conversion and Management*, vol. 34, issue 8, pp. 641-648, 1993.
6. S. E. Lyshevski, "High-power density mini-scale power generation and energy harvesting systems," *Energy Conversion and Management*, vol. 52, pp. 46-52, 2011.
7. P. C. Krause, O. Wasynczuk and S. D. Sudhoff, *Analysis of Electric Machinery*, IEEE Press, New York, 1995.
8. S. E. Lyshevski, *Electromechanical Systems, Electric Machines, and Applied Mechatronics*, CRC Press, Boca Raton, FL, 1999.
9. S. E. Lyshevski, *Electromechanical Systems and Devices*, CRC Press, Boca Raton, FL, 2008.
10. D. W. Hart, *Introduction to Power Electronics*, Prentice Hall, Upper Saddle River, NJ, 1997.
11. R. A. DeCarlo, S. H. Zak, and G. P. Matthews, "Variable structure control of nonlinear multivariable systems: A tutorial," *Proceedings of the IEEE*, vol. 76, no. 3, pp. 212-232, 1988.
12. S. V. Drakunov and V. I. Utkin, "Sliding mode control in dynamic systems," *Int. J. Control*, vol. 55, no. 4, pp. 1029-1037, 1992.
13. C. Edwards and S. Spurgeon, *Sliding Mode Control*, Taylor and Francis, Bristol, PA, 1998.
14. S. E. Lyshevski, *Control Systems Theory With Engineering Applications*, Birkhauser, Boston, MA, 2001.
15. A. S. Poznyak and Y. B. Shtessel, "Minimax sliding mode control with minimal-time reaching phase," *Proc. American Control Conference*, Denver, CO, vol. 1, pp. 174-179, 2003.
16. A. Levant, "Quasi-continuous high-order sliding-mode controllers," *IEEE Trans. Automatic Control*, vol. 50, no. 11, pp. 1812-1816, 2005.
17. Y. Shtessel, I. Shkolnikov and M. Brown, "An asymptotic second order smooth sliding mode control," *Asian Journal of Control*, vol. 5, no. 4, pp. 498-504, 2003.